A Critical Analysis of Brain Tumor MRI Segmentation and Classification Utilizing Machine Learning and Deep Learning Methods

Aruna V S, J. Vijayashree*
School of Computer Science and Engineering, Vellore Institute of Technology, Vellore
E-mail: aruna.vs2023@vitstudent.ac.in, vijayashree.j@vit.ac.in
*Corresponding author

Keywords: brain tumor, ischemic stroke, computer aided diagnostic, MRI, UNet, discrete wavelet transform (DWT) and residual network

Received: February 4, 2025

Brain Tumor (BT) result from uncontrolled cell growth and can be fatal if not treated. Classification and segmentation of data remain difficult despite many large-scale initiatives and encouraging results. Variations in the location, shape, and size of tumors make diagnosis difficult for doctors. This report provides a comprehensive literature analysis on magnetic resonance imaging (MRI) to aid researchers in detecting brain tumors (BT). The subject matter includes topics such as the anatomy of the Brain Tumor (BT), publicly available datasets, methods to improve the quality of images, dividing the tumor into distinct parts, extracting important characteristics, categorizing the tumor, using advanced Machine Learning (ML) techniques like Deep Learning (DL), transferring knowledge from one task to another, and employing fuzzy sets for analysis. The review provides an extensive overview of ML and DL methods for BT classification. With its capability to analyse vast amounts of data, DL has shown outstanding performance across various fields, particularly in biomedicine. This assessment offers comprehensive information about both 2-dimensional (2D) and 3-dimensional (3D) datasets and the methodologies used. The use and testing of MRI scans have been utilized to identify BT, resulting in positive outcomes. The goal of this study is to conduct a thorough and critical review of existing research on BT detection and classification using MRI.

Povzetek: Članek nudi poglobljen pregled naprednih metod strojnega in globokega učenja za MRI-segmentacijo in klasifikacijo možganskih tumorjev, ter izpostavi izzive, podatkovne nabore in smernice prihodnjega razvoja.

1 Introduction

As the brain and spinal cord facilitate dispersion, the Central Nervous System (CNS) conveys information about the body's senses and motor functions. The main brain components include the brain stem, cerebrum, and cerebellum. The typical male brain weighs 1.2-1.4 K and is 1260 cm3 and the female brain is 1130 cm3. Motor control, judgment, and problem-solving are all helped by the frontal lobe. The parietal lobe controls posture. The occipital governs vision, whereas the temporal handles memory and hearing. Neurons form a greyish cerebral cortex at the cerebrum's outermost section. The brain is bigger than the cerebellum. In neural-system animals, motor control organizes voluntary movements. Due to their changing size, stroke area and lesioning cannot detect tiny lesion patches. Human cerebellums are more developed than others. The cerebellum has three lobes: anterior, posterior, and flocculonodular. Each lobe is joined to the one behind it by the circular vermis. The greyish cortex and white matter (WM) core are thinner in the cerebellum than in the cerebrum. The anterior and posterior lobes collaborate to coordinate complex motor activities. The flocculonodular lobe keeps bodily processes in balance. The balancing act, breathing, and eye movement are regulated by peripheral and central nervous system bundles. From the brainstem to the spinal cord, thalamic nerves travel. All across the body, they were scattered. The medulla, pons, and midbrain comprise the brain stem. The midbrain facilitates ocular, muscular, auditory, and visual movements. While the pons regulates respiration, intra-brain communication, and sensations, the medulla oblongata regulates blood flow, swallowing, and sneezing [1]–[3].

The revolution in computer vision and ML has enabled the development of novel ideas and methods. Its applications in education, healthcare, and self-driving cars are just a few of the domains in which it has shown exceptional success [4]. Anomaly detection is one area where scientists have recently been focusing their attention on the biomedical applications of ML and Artificial Intelligence (AI) [5]. Automated, semi-automatic, or hybrid models that can accurately and quickly identify and segment tumors have been developed by researchers using DL [6] as a subfield of ML [7]. Since BT may vary greatly in size, form, location, and

appearance, radiologists still face challenges, even though early identification improves long-term survival and offers a more favourable prognosis. Doctors, patients, and researchers have already benefited from extensive work in this area. Although several Computer-Aided Diagnostic (CAD) systems have been developed to automatically detect and classify brain anomalies [8] and [9], there are still significant gaps in the field. Numerous evaluations have been published in this area, but none of them have addressed the shortcomings of the previous research or offered any noteworthy insights for the way forward. While deep models have the issue of gradient vanishing, hybrid models are not compatible with one another. The uniformity of data pre-processing is also deficient. To create a link across various methods, algorithms, and domains, DL optimization algorithms are needed. According to [7-9], the largest disadvantage of DL is its enormous annotated data need. The only way to find a solution to these issues is to conduct a comprehensive analysis of the methods already used and documented in the literature.

This study included current research articles that investigated the use of DL in identifying and categorizing BT from 2019 to 2024. The most recent cutting-edge studies on BT detection and categorization are what we want to review. The primary motivation for this study is our interest in working on a particular DL model known as multi-task learning. We also want to learn more about the weaknesses and vulnerabilities in current DL models so that we may better understand how to implement our suggested DL strategy.

The paper's structure is as follows: Section 1 serves as an introductory section of the study, while the second part 2 offers an in-depth elucidation of BT after the introduction. Section 3 of the report encompasses the literature review undertaken between 2019 and 2024. Topics covered include BT classifying and segmenting using various ML and DL methods, datasets, and performance indicators. Section 4 provides a comprehensive analysis of this work, including its drawbacks. Section 5 presents the study's conclusion, while Part 6 provides the sources used in this work.

Brain tumor

BT are categorized as either aggressive or slow-growing. A malignant tumor, characterized by its aggressive nature, can metastasize and spread from its initial place to many organs and tissues. In contrast, a benign tumor, which grows at a slower pace, does not invade or infiltrate the surrounding tissues [10]. As far as the World Health Organization (WHO) is concerned, BT falls within categories I–IV [11], [12]. Grades III and IV malignancies are characterized by their high aggressiveness and poor prognosis, while malignancies of grades I and II are thought to advance slower. The details about the grading of BT are outlined below [13], [14].

Grade I: Cancers are characterized by their sluggish growth and low tendency to spread. These may be effectively removed by surgical procedures and have been associated with enhanced duration of survival. Grade 1 pilocytic astrocytoma is one sort of this tumor.

Grade II: Cancers have a sluggish growth rate, but possess the capability to metastasize to other tissues and progress into tumors of a higher grade. Despite undergoing surgical intervention, several types of malignancies have the potential to reoccur. Oligodendroglioma is a kind of this type of tumor.

Grade III: Tumors can invade neighbouring tissues and have a faster growth rate compared to grade II tumors. For certain types of malignancies, surgical intervention alone is insufficient; postoperative chemotherapy or radiation treatment is offered. One particular instance of this kind of tumor is an anaplastic astrocytoma.

Grade IV: Tumors are characterized by their high aggressiveness and ability to spread rapidly. They could use blood vessels to expedite their development.

Ischemic stroke: An ischemic stroke occurs when the brain's blood flow is interrupted. An ischemic stroke occurs when the blood supply to a portion of the brain is cut off, depriving the tissue of enough oxygen and hastening the process of death. Context Globally, ischemic stroke is a leading cause of mortality and disability. Lesions related to strokes are classified as acute (0–24 hours), sub-acute (1–2 weeks), and chronic (since more than 2 weeks ago).

A BT results from the uncontrolled development of both living and dead brain cells. Disease size and severity affect BT survival. Primary and secondary BT differ in genesis. Secondary tumors travel to the brain from the outside, whereas primary brain malignancies start within [15]. The soft tissue composition of the three components and tumor exhibit varying contrasts under various physical conditions, rendering them crucial for the identification of BT in MRI imaging. T1, T2, T1-CE, and Fluid Attenuation Inversion Recovery (FLAIR) have frequently used MRI images [16], [17] as shown in Figure 1.

T1-weighted images: In T1-weighted imaging, cerebrospinal fluid (CSF) appears as a dark color, whereas MRI reveals adipose tissue.

T2-weighted images: Prolonged lengths of Repetition Time (TR) and Time to Echo (TE) result in increased brightness of CSF. These images depict the distribution of adipose tissue and hydration levels throughout the body.

T1-CE images: While the TE and TR are identical to those of T1 images, these images are taken after injecting a non-toxic gadolinium contrast agent. The agent can light imaging locations.

FLAIR images: By using extended TE and TR values, FLAIR images are acquired. By doing this action, any irregularities stay visible while the normal CSF appears black. This sequence is prone to sickness, which facilitates the differentiation of CSF and abnormalities [5], [18].

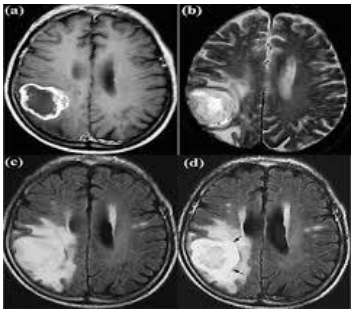

Figure 1: The imaging modalities used in this case are a. T1 Weighted, b. T2 Weighted, c. FLAIR, and d. FLAIR with contrast enhancement (https://bit.ly/33ab5og)

Brain imaging modalities

Medical imaging remains the most efficient approach for discovering, evaluating, and diagnosing gliomas and other medical conditions. Computerized Tomography (CT), positron emission tomography, MRI, functional magnetic resonance imaging, and Diffusion Tensor Imaging (DTI) are the imaging modalities most often used in clinical settings. While each of these methods has its own set of benefits, they may all be combined to create a more comprehensive view. Mathematical models may be used to predict the progression of BT over time by using many time points of various modalities. Growth prediction has special importance as it may provide valuable insights into the tumor's physiology, aid in measuring the tumor's aggressiveness, enhance treatment planning, and perhaps even forecast the patients' survival in the context of precision medicine [19].

The evaluation of medical data was performed by using ML and DL techniques, applying the following methods:

MRI: To acquire electromagnetic signals, magnetic resonance is used. These signals are produced by human organs, which helps us reconstruct further details on the anatomy of human organs. High-resolution MRIs include more structural features that are necessary for identifying lesions and diagnosing diseases.

CT-Scan: This technique uses digital geometry to create 3-D images from 2-D X-ray images.

Mammogram: Mammograms are used for early identification of anomalies in the body and the successful screening of breast cancer. Masses and calcifications are thought to be the most typical abnormalities that lead to breast cancer.

Electrocardiogram (ECG): This device measures electrical heart activity and helps identify cardiac issues in people [20].

Out of all these technologies, MRI is the most superior technology for researching the brain due to its ability to accurately identify tissues with a high level of spatial resolution. The same tissue area may be represented by many images using varying contrast visualizations. These several imaging types may provide very helpful information for the same area, assisting researchers in accurately studying brain disease. It is effective in tumor identification, as it is a non-invasive technique without producing harmful radiation [21].

2 Literature review

The increasing complexity of Cyber-Physical Reviewing various works in the area of DL and ML applications for medical imaging is the main objective of this research. Classification, detection, and segmentation are critical tasks in medical image processing. To train and complete specific DL tasks in medical applications, deep neural networks need large amounts of labelled data. Nonetheless, the medical field is lacking of annotated data points. Transfer Learning (TL) is one tactic to address this problem. Fine-tuning a pre-trained network and fixed feature extractors are two popular and widely utilized TL approaches. The classification method divides images into two or more classes using DL models. In the process of detecting anomalies in medical imaging, DL algorithms identify organs. The models attempt to separate medical image regions of interest for processing in the segmentation challenge [22]. DL can also extract complicated features that humans cannot see, allowing quantified image interpretation [23].

Fuzzy C means feature extraction methods, neural networks, and mathematical morphology were introduced for better performance [24], [25]. Also, an evolutionary algorithm is important in medical image analysis. Genetic algorithms are employed to identify glioma grades noninvasively. It is used to select and optimize features [26], suggested by utilizing MRI [27] and spontaneous categorization to improve accuracy. We find the best features in the dataset using Swarm Intelligent Redundancy Relevance (SIRR) [28]. In the paper [29], the enormous data collection is decreased in dimension using the evolutionary correlated gravitational search method, an excellent optimization strategy.

The research articles that discuss the segmentation and classification of BT MRI images using ML and DL approaches are thoroughly reviewed in this part and span the years 2018 through 2024. This section's format is as follows: We conduct a thorough assessment of the majority of articles that deal with the ML and DL techniques used to separate BT from MRI images, along with the datasets and performance metrics used in each. Most papers use ML and DL techniques to classify MRI images as BT. The classification is shown in Figure 2 and the table along with the datasets and performance metrics used in the examined research papers.

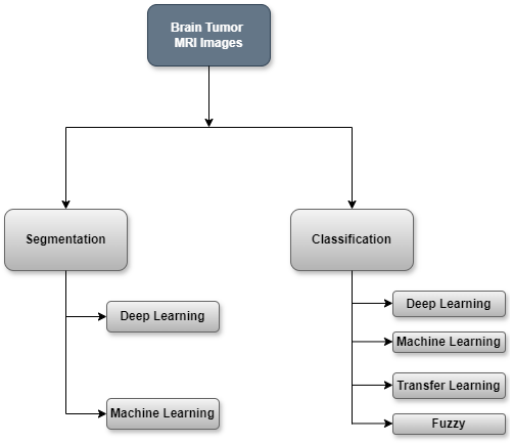

Figure 2: Different methods used in BT classification

2.1 Segmentation of brain tumor using different methods

Automated BT segmentation is essential for computer-aided glioma diagnosis. Automating these procedures could potentially enhance their effectiveness and efficiency. This study presents a hybrid method for segmenting BT. To segment MRI in the BRATS 2013 dataset, the hybrid model makes use of Deep Convolutional Neural Networks (DCNNs) and multimodal MRI data. The hybrid model, which included two-path Convolutional Neural Networks (CNNs) and three-path CNNs, surpassed cutting-edge methods in every significant performance criterion. Using a patch model, the suggested network segments the brain anatomy by classifying the core pixels of individual patches. They slice the 3D MRI into 2D spatial layers. It uses local and global data to predict output classes, considering label correlations between pixels. The training technique for the model is two-phase to ensure precise label distribution and manage inconsistent data [30]. BT exhibits significant variation in terms of their size, shape, and overall appearance, posing challenges in their identification. This study classifies input slices as either healthy or sick (tumor) using a DL network. In this work, a high-pass filter image fused with the input slices highlights the inhomogeneity field impact of the magnetic resonance slices. The fused slices also go through the median filtering procedure. It is easy to enhance the output slices by simply smoothing and emphasizing the borders of the input slices. Subsequently, the 4-connected seed-generating algorithm categorizes pixels with comparable intensity from the input slices. Then, refine the segmented slices into the Stacked Sparse Auto Encoder (SSAE) model using two layers of a recommended stacked sparse autoencoder. The author selected the model's hyperparameters after extensive testing. In the first layer, they use 200 hidden units, and in the second, 400. Evaluated the prediction of images with and without tumors on the softmax layer [31].

Due to the high labour and time requirements of manual segmentation, automatic segmentation is the superior method. When it comes to medical picture segmentation, the UNet is a popular and versatile architecture. For 2D and 3D medical picture segmentation, this paper suggests and applies 2DGA-UNet and 3DGA-UNet, respectively. The initial version uses TL and UNet architecture to improve the 2DGA-UNet framework's performance. Visual Geometry Group 16 (VGG-16), a collection of basic CNN, encodes the 2DGA-UNet network. In 3DGA-UNet, up-sampling operators replace pooling operators, adding layers to a large contractual network. Consequently, these layers can learn from a limited number of images and surpass current best practices with output resolution. These models evaluate their performance on five benchmark datasets as mentioned in Table 1. The findings demonstrate excellent performance across 14 medical image segmentation assessment factors. From the comparison of performance metrics given in Table 3, the GA-UNet performs better than conventional approaches [32]. This paper introduces a novel cloud-based 3D U-Net method for BT segmentation, which makes use of the BRATS dataset. In this research, we look into how the 3-D U-Net network deviates when max pooling layers and convolutional layer initial sequences are combined. Cloud computing has several benefits. This network's worldwide accessibility reduces computational expenses. It effectively trained the system using the many hyperparameters of the Adam optimization solver. We provide the first cloud-based method with an average dice score of 95% that achieves maximal accuracy. Then the dice score is calculated using the Sorensen similarity coefficient [33]. In another article, the author proposes a fully automated approach utilizing the BraTS2020 dataset and 2D U-net design for tumor localization separation from normal tissue. Each distinct MRI sequence serves as training data to retrieve (Region of Interest) ROIs, or tumor regions in brain MRIs. To save computational costs, the input image graphs are reduced in size to a single 128 by 128 images, and then normalized. We evaluate the model using all MRI sequences to determine which yields the highest performance [34].

An attention module named Attention Gate was developed and its efficacy for BT segmentation was the intended focus of this study. The Attention Gate Residual U-Net (AGResU-Net) architecture incorporates attention gates and residual modules into an original, simplistic U-Net design. It augments the skip connection with several attention gate units to focus on relevant feature data and ignore irrelevant or noisy feature replies. Not only does AGResU-Net collect large amounts of semantic data to improve feature learning, but it also manages data on small-scale BT. We do a comprehensive evaluation of attention gate units using three reliable MRI BT benchmarks. Evidence from experiments shows that AGResU-Net and AGU-Net perform better than their respective baselines, ResU-Net and U-Net [35]. A DWT and a Daubechies wavelet kernel are used throughout the fusion process to provide a more informative tumor region than a single, independent MRI signal. After fusion is complete, noise is removed using a Partial Differential Diffusion Filter (PDDF). A suggested CNN model is fed to the segmented tumor region using a global thresholding strategy to discriminate between tumor and non-tumor regions. To evaluate the suggested technique, five datasets that are publicly accessible are used. The results show that fused images perform better than isolated sequences on benchmark datasets [16]. Early diagnosis of BT may lead to patient survival. This study proposes to segment lesion symptoms properly using the Grab Cut technique and refine the TL model VGG-19 by extracting features that are sequentially combined with manually generated (shape and texture) data. Classifiers get a fused vector as a result of entropy's optimization of these characteristics for quick and precise classification. They evaluated the suggested method using three years' worth of multimodal BT segmentation BRATS challenge datasets from the top Medical Image Computing and Computer-Assisted Intervention (MICCAI) competitions. They test and train the suggested approach on benchmark datasets like BRATS 2015–17. The highest possible results on the BRATS 2015 exam are DSC = 0.9636 and accuracy =

0.9878. In 2016, we achieved a DSC of 0.9959 and an accuracy of 0.9963, while in 2017, we achieved a DSC of 0.9967 and an accuracy of 0.9980 [11].

Tumor segmentation and grading are commonly used for MRI and are crucial for diagnosing and formulating a treatment strategy. They developed a DL approach using CNNs built with U-net and TL, a fully connected classifier for grading, and a pre-trained VGG-16 convolution basis to meet the clinical need for tumor segmentation. We train and assess the segmentation and grading models using T1-precontrast, T1-postcontrast, and FLAIR MRI data from 110 patients diagnosed with Lower-Grade Glioma (LGG). The segmentation model has an average DSC of 0.84 and an accuracy of 0.92 in identifying tumors [36]. We talk about a way to use CNN to automatically tell the difference between BT in 3D BT Segmentation. Furthermore, we used whole-brain 3D imaging to compare predicted labelling in three dimensions with ground truth. The method used sagittal, coronal, and axial images to accurately establish the position and dimensions of the tumor, including its height, width, and depth. Tumor prediction outcomes via semantic segmentation with a DL network are promising. 91.718 was the average prediction ratio [37].

Table 1: Summary of methods and datasets used for brain lesion segmentation and classification

Ref.	Method	Dataset
[30]	-CNN with two paths -CNN with three paths - Hybrid CNN	BRATS 2013 Dataset (3D images)
[31]	- Lesion Enhancement Using High Pass Filter - Lesion Segmentation Using Seed Growing Method -Autoencoders (AE) -Sparse Autoencoder (SAE) - Stack Sparse Autoencoder	A few examples of BRATS datasets: 2012 (challenge and synthetic), 2013 (and 2013 Leaderboard), 2014, and 2015 datasets
[32]	- Two variants of GA-UNet: 2DGA-UNet and 3DGA-UNet - TL with VGG16 - encoder in 2DGA-UNet - Up sampling operators replacing pooling operators in 3DGA-UNet	- Brain lesion segmentation (MICCAI 2008 Multiple Sclerosis Challenge) - BRATS 2018 and BRATS 2019 - Lung segmentation - Segmentation of the liver (3D-IRCADb database)
[33]	Segmentation method: 3D U-Net	BraTS 2020 3D
[34]	U-Net	BraTS 2020
[35]	AGResU-Net model	BRATS 2018, 2019, and BRATS 2017
[16]	CNN, PDDF, Daubechies wavelet kernel, and DWT	BRATS Leader Board, BRATS 2012, 2013, 2015, and 2018
[11]	Grab cut technique, VGG 19, and manually created feature extraction using HOG (Histogram of Oriented Gradients) and LBP (Local Binary Pattern)	BRATS 2015, 2016, and 2017
[36]	A pre-trained VGG16, fully connected classifier for segmenting and U-Net	The Cancer Imaging Archive (TCIA)
[37]	Semantic segmentation - CNN	BRATS dataset 3D
[38]	3D fully CNN	BRATS 19 and 2018 datasets
[39]	3D U-Net	BT classification using MRI data from Kaggle
[40]	The Fully Resolution Convolutional Network (FrCN), the MSFO method, and the LBM	BRATS 18, BRATS 19, BRATS 20

The datasets used in the various kinds of research publications are shown in Table 2 below. Additionally, the size of the dataset, whether it was composed of 3D or 2D MRI images and the modalities of the datasets are discussed.

Table 2: Segmentation of BT MRI different datasets

Ref.	Dataset	Dataset Size	Modalities and Dimension
[30]	BRATS 2013 Dataset (3D images)	3D images: HGG - 20, LGG - 10; 2D slices - 155	MRI Modalities: T1, T2, T1c, T2FLAIR
[31]	BRATS Challenge and Leaderboard (2012-2015)	Each case has 155 slices; Cases: • 2012: LGG - 25, HGG – 25 • 2012 Synthetic: LGG - 25, HGG – 25 • 2013: LGG - 10, HGG - 20 • 2013 Leaderboard: LGG - 4, HGG – 21	---

		• 2014: LGG & HGG – 200 • 2015: LGG - 54, HGG - 220	
[32]	Brats'18 & Brats'19, Lung Segmentation, 3D-IRCADb-01	Brats'18: 285 cases (HGG - 210, LGG - 75) Brats'19: 285 cases (HGG - 210, LGG - 75) Lung Segmentation: Shenzhen dataset (336 normal, 326 abnormal CXR of TB), Chest X-ray (112,120 Frontal CXR), RSNA pneumonia detection challenge (30,000 exams) 3D-IRCADb-01: 3D CT scan (20 patients, 15 hepatic tumors)	Brats'18: Volumes from structural MRI (T1, T1Gd, T2, T2-FLAIR)
[33]	Brats 2020 (3D)	7 GB, 750 MRI scans of brain tumors Training: 484 labeled voxels Test: 266 label-free volumes	240 × 240 × 155 × 4 Modalities: FLAIR, T1w, T1gd, T2w
[34]	BraTS 2020	473 subjects, 5 images per subject	Dimension: 224 × 224 × 150 Modalities: FLAIR, T1, T1ce, T2, Seg
[35]	BraTS 2017, 2018, 2019	Brats 2017: Training - 285 cases (HGG - 210, LGG - 75), Validation - 46 cases Brats 2018: Training - 285 cases (HGG - 210, LGG - 75), Validation - 66 unlabeled cases Brats 2019: Training - 335 cases (HGG - 259, LGG - 76), Validation - 125 cases	MRI Modalities: T1, T2, T1c, T2FLAIR
[16]	BRATS Leaderboard (2012-2018)	Brats 2012: HGG - 10, LGG – 5 Brats 2013: HGG - 20, LGG – 10 Brats 2013 Leaderboard: HGG - 21, LGG – 4 Brats 2015: 384 cases (Training: HGG - 220, LGG - 54; Testing: 110 cases) Brats 2018: HGG - 191, LGG - 75	Flair, T1, (Flair + T1) MRI sequences
[11]	BRATS 2015, 2016, 2017	BRATS 2015: Training - (HGG - 220, LGG – 54), Testing - 110 cases BRATS 2016: Training - (HGG - 220, LGG - 54) BRATS 2017: Training - (HGG - 210, LGG - 72) High & Low-grade images: HGG - 130,200, LGG - 46,500 Normal & Glioma images: Glioma - 15,272, Non-glioma - 19,032	BRATS 2015 Challenge: 240 x 240 x 155 x 4 (155 slices in each scenario) Modalities: Flair, T1, T1c, T2
[36]	The Cancer Imaging Archive (TCIA)	3,929 images (Tumor: 1,373, Tumor-free: 2,556)	MRI sequences: T1 pre-contrast, FLAIR, T1 post-contrast Includes patient data (tumor grade, subtype, gender, age)
[37]	BraTS dataset	Training: 257 labeled images Testing: 5 distinct images	Dimensions: 240 × 240, 155 slices Modalities: T1, T1C, T2, FLAIR
[38]	BraTS 2019 & 2018 datasets	BraTS 2019: 462 MRI scans Training: HGG - 259, LGG – 76 Validation: 127 cases BraTS 2018: Validation - 67 MRI scans	Modalities: FLAIR, T1, T1c, T2
[39]	Kaggle dataset for BT classification	3,264 files (Training & Research set)	Classification: Pituitary, Meningioma, Glioma, Absence of tumor
[40]	Brats'18, Brats'19, Brats'20	Brats'18: HGG - 191, LGG - 75 Brats'19: 335 cases (HGG - 259, LGG - 76) Brats'20: 494 cases (Training - 369, Testing - 125)	---

The performance metrics for evaluating the MRI BT include the Dice score, sensitivity (SE), specificity (SP), accuracy (ACC), Jaccard Similarity Index (JSI), False Negative Rate (FNR), False Positive Rate (FPR), Area Under the Curve (AUC), Positive Predictive Value (PPV), Highest Density Intervals (Hdis), Variable Speed Drives (VSds), Lesion True Positive Rate (LTPR), Lesion False Positive Rate (LFPR), True Positive (TP), True Negative (TN), False Positive (FP), False Negative (FN), and Precision (PREC). These metrics are presented in Table 3.

Table 3: Segmentation performance metrics in BT magnetic resonance imaging (BT MRI)

Ref	Modality	Dice	SE	SP	ACC	JSI	FNR	AUC	PPV	FPR
[30]	Complete	0.86	0.86	0.91	-	-	-	-	-	-
	Core	0.86	0.87	0.93	-	-	-	-	-	-
	Enhancing	0.88	0.90	0.94	-	-	-	-	-	-
[31]	2012	1.00	1.00	1.00	100	1.00	0.00	1.00	1.00	0.00
	2012 Synthetic	0.94	0.88	1.00	90	0.89	0.12	1.00	1.00	0.00
	2013	0.96	1.00	0.90	95	0.93	0.00	0.97	0.93	0.10
	2013 Leaderboard	1.00	1.00	1.00	100	1.00	0.00	1.00	1.00	0.00
	2014	0.98	0.98	0.96	97	0.97	0.02	0.99	0.98	0.04
	2015	0.96	0.93	1.00	95	0.93	0.07	0.96	1.00	0.00
[32]	BraTS'18	92.1	95.5	92.1	-	-	-	-	-	-
	BraTS'19	90.29	93.27	92.0	-	-	-	-	-	-
	MICCAI 2008	99.4	99.6	64.0	-	-	-	-	-	-
	Lung	98.35	97.7	95.1	98.4	-	-	-	-	-
	Liver	81.2	81.3	99.1	90.2	-	-	-	-	-
[33]	BraTS'22	0.95	-	-	-	-	-	-	-	-
[34]	FLAIR	91.23	98.53	99.14	98.95	93.9	-	-	-	-
	T1	93.86	98.97	99.68	99.41	-	-	-	-	-
	T1ce	85.67	98.72	98.52	98.68	-	-	-	-	-
	T2	79.32	98.49	98.37	98.25	-	-	-	-	-
[35]	BraTS'17	0.749	-	-	-	-	-	-	-	-
	BraTS'18	0.772	-	-	-	-	-	-	-	-
	BraTS'19	0.709	-	-	-	-	-	-	-	-
[16]	BraTS'18 (Flair)	0.96	-	-	-	-	-	-	-	-
	BraTS'15 (T1)	0.82	-	-	-	-	-	-	-	-
	BraTS'18 (T1C)	0.20	-	-	-	-	-	-	-	-
	BraTS'18 (T2)	1.00	-	-	-	-	-	-	-	-
	BraTS'18 (T1C+T2)	0.95	-	-	-	-	-	-	-	-

2.2 Deep learning

To efficiently integrate both local and global contextual information, the suggested design makes use of a deep neural network and a 3D convolutional layer, giving lower weights to each. This is achieved by the use of minuscule kernels. To overcome the data's intrinsic unpredictability, the author suggested a preprocessing method for MRI that makes use of adaptive contrast augmentation and intensity normalization. In addition, a data augmentation strategy was used to ensure that the robust 3D network was trained effectively [43]. To classify the medical images, we use a CNN feature combination with SVM. The Figshare public dataset, including MRI images of three distinct types of BT, is used to evaluate the fully automated methodology. CNN is designed to extract features from brain MRI scans. CNN characteristics are combined with a multiclass SVM for improved performance. The integrated system underwent testing and evaluation using a five-fold cross-validation procedure. With an accuracy rate for classification of 95.82%, the suggested model outperformed the most advanced method. The proposed approach is tested extensively on other brain MRI datasets to determine its efficacy [44]. An efficient DL method for multiclass brain cancer categorization is presented in this study. The Densenet201 Pre-Trained DL Model is adjusted and refined utilizing unbalanced data via deep transfer. Each tumor type is covered by the average pooling layer, which extracts the trained model's properties. Two feature selection methods are used since this layer's properties are unsuitable for exact categorization. Two methods are discussed: Entropy-Kurtosis-based High Feature Values (EKbHFV) and Metaheuristic-based Modified Genetic Algorithms (MGAs). Our threshold function improves Genetic Algorithm (GA) properties. Finally, a non-redundant serial-based technique combines and classifies EKbHFV and MGA characteristics by using a multiclass SVM cubic classifier. This method employed BRATS 2018 and BRATS 2019 without augmentation and obtained over 95% accuracy [45].

CNN multi-classifies BT for early detection. Three CNN models for classification tasks are shown. Grid

search optimization finds all CNN model hyperparameters automatically. This CNN multi-classification of BT MRI images tunes most hyper-parameters using the grid search optimizer [46]. A powerful DL strategy for BT classification utilizing many data sources is presented in this research. To begin, a nine-layer CNN model is trained to enhance contrast using a combination of hybrid division histogram equalization and ant colony optimization. Moth flame and differential evolution optimize characteristics from the second completely connected layer. Both algorithms' results are blended using matrix length and delivered to MC-SVM. In experiments, the recommended strategy obtained 99.06, 98.76, 98.18, and 94.6% accuracy on BRATS 2013, 2015, 2017, and 2018. Results indicate that greater tumor visualization before CNN model training leads to improved feature generation. Feature optimization affects processing time, whereas fusion results in increased accuracy and time [47]. To get three-dimensional brain lesions, this research expands 2D-CNNs to multimodal 3D-CNNs. It can resolve the wide neighbourhood of errors that the 2D-CNNs raw input demands while also extracting the modalities of the information differences more effectively. Next, to accelerate the network's convergence and reduce over-tipping, the true normalization layer is inserted in between the pooling and convolution layers. Finally, by using the weighted loss function, we were able to adjust the loss function and improve the feature learning in the lesion region [48].

This research divides BT into two categories using three BraTS datasets, with four 3D MRI sequences per subject in each dataset and uses two methods. As a service, they provide a hybrid model that combines 3D CNNs with long short-term memory (LSTM): TD-CNN-LSTM. On every tier of this paradigm, Time Distributed functions are embedded. The goal is to combine all four MRI scans of every patient into one input dataset since they all provide important information about the tumor. Hence, the model is fine-tuned for layer design and hyper-parameter selection via ablation studies. In the second part, they use each MRI sequence to build a 3D CNN model, which we then use to evaluate performance. Additionally, datasets undergo preprocessing for optimal performance. In tests, the TD-CNN-LSTM network achieved the best accuracy of 98.90%, surpassing 3D CNN [49]. The researchers introduced an innovative BT classification technique using DL, which operates across many grades. The methodology we employ consists of three main steps. Firstly, they utilized a CNN model to separate the tumor areas from the dataset. The second step is to improve the segmented data by adding more parameters to increase the sample size. Lastly, BT is divided into several categories by refining a pre-trained VGG-19 CNN model. By using DL and data augmentation, they enhanced the precision of the proposed technique. The findings of the trial demonstrate how well the suggested CNN-based CAD system works to support radiologists in making accurate decisions while grading multi-grade BT into four categories [50]. In this article the author uses a 3D-CNN to categorize brain MRI images into two predetermined categories. Furthermore, they suggest visualizing the 3D-CNN's behaviour using a Genetic Algorithm-based Brain Masking (GABM) method to get a new understanding of its operation. Two separate steps to the GABM method have been suggested. Firstly, the 3D-CNN is trained using brain MRI data. The second step is using a GA to identify brain regions in MRI data. The 3D-CNN primarily extracts crucial and discriminative characteristics from the knowing areas of the brain [51].

The research introduces a more advanced methodology for classifying brain tumors using MRI data. The suggested technique employed a Residual Network (ResNet), a DL architecture, to build the model. To expand the dataset and improve accuracy, we used rotating, shifting, zooming, vertical and horizontal flips, brightness, shearing, and ZCA whitening change [52]. The author introduced A CNN architecture, which then used a U-Net-based model to separate brain pictures and classify them into four distinct groups. The author used six standardized datasets to test and train the classification and segmentation models to determine how segmentation affects brain MRI tumor categorization. While testing on all six datasets, our one-of-a-kind deep-learning BT segmentation and classification model outperformed pre-trained methods [53]. By including adjacent tissues in the tumor area (ROI expansion), characteristics may become more apparent. This study utilizes pre-trained AlexNet (Alexnet, a previous deep CNN approach, significantly improves ImageNet classification [54]), ResNet-18, GoogLeNet, and ShuffleNet to extract deep characteristics from tumors and surrounding tissues. Deep features are crucial to tumor classification, but as the network gets more complicated, it may forfeit low-level information. Shallow neural networks handle fundamental data. After that, deep and superficial traits are blended to compensate for information loss [55].

They present an automated brain illness diagnosis model utilizing computer vision based on exemplars. The model produces profound characteristics by using exemplars. Choose a pre-trained DL model for generating features. The selected feature extractor is MobilNetV2. The automated brain sickness detection model consists of four stages: preprocessing, production of example deep features, Iterative Neighbourhood Component Analysis (INCA) feature selection, and SVM classification. During the processing phase, the original brain scans are scaled down to dimensions of 512 × 512 and then divided into two sets of exemplars, one with dimensions of 128 × 128 and the other with dimensions of 256 × 256. MobileNetV2 generates 1000 features from each example and scaled image. The INCA feature selector takes all of the extracted features that were created and chooses the best one. The SVM classifier uses the chosen feature as input [56]. This article presents a novel approach using a CNN, together with conventional classifiers and DL approaches, to accurately differentiate brain cancers from 2D MRI. To train the model efficiently, they have obtained a diverse collection of MRI scans that include several tumors with varying sizes, forms, locations, and levels of picture intensity. To verify the accuracy of this work, we have used the SVM classifier as well as different activation algorithms including sigmoid, softmax, and RMSProp.

We use the Python programming language, using "TensorFlow" and "Keras", to develop our recommended solution due to its efficiency and effectiveness. CNN achieved 99.74% accuracy in our work [57].

This study suggests automated categorization for fast, accurate diagnosis. This is believed to be the first two-stage deep CNN model capable of accurately classifying three distinct tumor kinds as well as typical brain cell. The best CNN models and classifiers were evaluated using a two-stage ensemble and classification method to ensure the model's correctness. The model's functionality is enhanced by a two-stage ensemble that incorporates Principal Component Analysis (PCA) and data augmentation. The two-stage ensemble boosts accuracy 4.31%. PCA reduces execution time by 6.71 and features by 18.71 [58]. For real-world use, models are inadequate as they rely on the most precise tumor model derived from slices. This research introduces a new 3 (Attention-Convolutional-LSTM) DL model for classifying BT using MRI data. All three ACL models integrate attention, convolutional, and Long Short-Term Memory (LSTM) structures into a single learning framework, using an end-to-end learning technique. Because of this, the ability to mirror the attributes was improved. Due of the three-dimensional nature of the model, the 3ACL model made direct use of three-dimensional MRIs without first converting them to two-dimensional data. Deep, very representative features are generated by the 3ACL model's fully linked layer. A set of features is sent into the SVM. The classification accuracy was further enhanced by including expected outcomes from all SVM slices into the weighted majority vote technique [59].

2.3 Machine learning

The approach proposed for BT detection produces efficient and improved results. To make the overall system more efficient, each of the various activities, such as pre-processing, segmentation, and feature extraction, among others, collaborate. The use of these pre-processing approaches allows for the achievement of favourable outcomes in segmentation, which in turn assists in the extraction of certain characteristics that are correct for classification. Attained a 95.85% accuracy rate with the use of a watershed technique combined with SVM classification [42]. The next article describes MRI brain cancer detection ML. Optimization selects traits to reduce duplication and boost relevance. Pre-processing NMF lowers brain MRI noise; Segmentation enhances tumor identification. GLCM and spatial Gray level dependence matrix (SGLDM) extract key attributes from MRI-smoothed images. Select meta-heuristic Harris Hawks Optimization (HHO) properties alone. The Knowledge-based Support Vector Machine (KSVM) classifier, which is based on ML, categorizes MRI images as either benign or malignant depending on certain factors [24].

ML-Based Back Propagation Neural Networks (MLBPNN) improve pathologists' danger location accuracy and reduce entomb onlooker variability in BT categorization. Acquisition, upgrading, division, extraction, image portrayal, characterization, and leadership are needed to prepare biopsy images for disease localization. This study analyses MLBPNN using infrared sensors. Subsystem reduction simplifies the neural distinguishing proof calculation. Fractal dimension technique uses multi-fractal detection to find the most relevant characteristics to simplify the process. The wireless infrared imaging sensor delivers tumor warming data to a specialist doctor for general health monitoring and ultrasound measurement management, particularly for elderly faraway patients [60].

2.4 Transfer learning

This paper [61] proposes a new approach for categorizing images of BT using a strategy that combines fine-tuning with TL. Utilizing a pre-trained CNN as a readily available tool for extracting features, without the need for additional training, to train a separate classification method (such as KNN, SVM, Boosted Trees, DTs, and Random Forest) is distinct from the suggested approach of TL with block-wise fine-tuning. We suggest using a TL method that makes use of a deep CNN model that has already been trained and then fine-tuning it block-wise. Using the T1-weighted contrast-enhanced MRI (CE-MRI) benchmark dataset, the suggested method is assessed. This study [62] introduces a novel tumor detection approach. The suggested approach consists of four steps: normalization, segmentation, classification, and fusion of the scores obtained from the Alex/Google DL model using MRI/CT modalities. With its score-based fusion method, the whole tumor area may be precisely segmented and classified.

2.5 Fuzzy

This study seeks to construct a brain cancer classifier using smart segmentation and classification. The recommended method incorporates data collection, preprocessing, tumor segmentation, and classification. Benchmark BT datasets are pre-processed. Here, median filtering and contrast enhancement are used. The Adaptive Fuzzy Deformable Fusion (AFDF) method integrates Fuzzy C-Means Clustering (FCM) with snake deformable approaches for segmentation. This scenario utilizes the updated Deer Hunting Optimization Algorithm (DHOA), commonly referred to as Adaptive Coefficient Vector-based DHOA, to improve crucial AFDF parameters. An ensemble classifier consisting of an autoencoder, SVM, and Deep Neural Network is suggested as a replacement for the fully connected layer in DL classification. ACV-DHOA optimizes CNN's hidden and convolutional layers [63]. This paper suggests a Neutrosophy-CNN hybrid approach. It classifies brain-image-segmented tumor regions as benign or malignant. They started by segmenting the MRI images using the Neutrosophic Set-Expert Maximum Fuzzy-Sure Entropy (NS-EMFSE) method. Segmented brain pictures were classified using CNN features using SVM and KNN classifiers. The experimental evaluation included doing a 5-fold cross-validation on a dataset consisting of 80 noncancerous tumors and 80 cancerous tumors. The research shows that CNN features surpassed many classifiers in the task of

classification [64]. As shown in Figure 3, the image that was chosen is used for the various classifications of the procedure. The procedure for classifying BT is further upon in Table 4, which includes several different approaches.

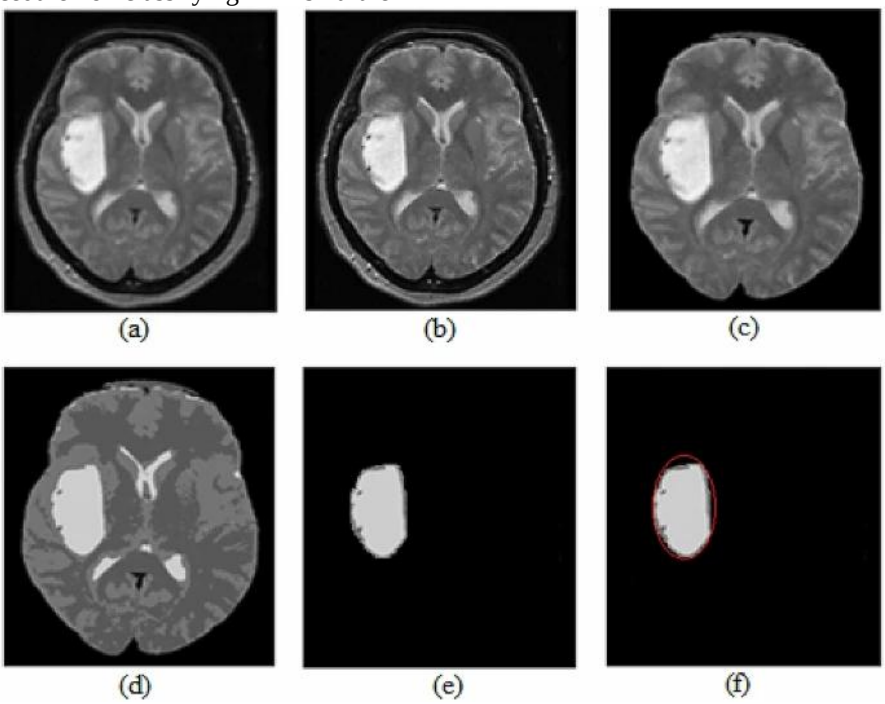

Figure 3: a) The Original Picture, b) Refined Picture c) Picture with Removed Skull, d) Image with Segmented Regions, e) Region of Tumor, f) Extracted Tumor Region [65]

Table 4: Classification of BT MRI Using Different Methods

S. No	Method	Dataset
[43]	3D CNN	BraTS 2018
[44]	CNN features with SVM	Dataset 1 (2018) - Figshare, Dataset 2 (2019) - Radiopaedia, Dataset 3 (2019) - Harvard University
[45]	Densenet201, EKbHFV, MGA	BRATS 2018, BRATS 2019
[46]	CNN with Fully Optimized Framework	RIDER, REMBRANDT, TCGA-LGG
[47]	DL Network	BraTS 2013, 2015, 2017, 2018
[48]	3D-CNN with multi-modal input	MICCAI BraTS 2018
[49]	Time Distributed-CNN-LSTM	BraTS 2018, 2019, 2020 (3D images)
[50]	Deep CNN with VGG-19 and data augmentation	Radiopaedia dataset, BT dataset
[51]	3D-CNN and GABM	ADNI (Alzheimer's Disease), ABIDE (Autism Brain Imaging Data Exchange)
[52]	ResNet	3,064 BT MRI images (2005–2010) from Nanfang Hospital (Guangzhou) & General Hospital (Tianjing Medical University)
[53]	VGG16, VGG19, EfficientNet B0, EfficientNet B7, ResNet152V2	Sets A, B, C, D
[55]	AlexNet, ResNet-18, GoogLeNet, ShuffleNet; SVM, k-NN classifiers	BT dataset, LGG-1p19q Deletion Dataset
[56]	MobileNetV2, Exemplar deep feature generator, INCA, SVM	Firat University Hospital Radiology Department dataset
[57]	CNN	BraTS 2020
[58]	Feature Extractors: Modified VGG-19, EfficientNet-B0, Inception-V3, ResNet-50, Xception; Classifiers: SVM, RF, KNN, AdaBoost, PCA	Sets 1, 2, 3, combined datasets
[59]	3ACL (Attention-Convolutional-LSTM) DL model	BraTS 2015 & 2018 benchmark datasets

[42]	SVM, KNN, Tree, Ensemble, Logistic Regression	Private dataset (512 images, Nishtar Hospital, Multan, Pakistan), Slice-based dataset (940 images)
[24]	Binomial Thresholding, GLCM, SGLDM, HHO, Kernel SVM	BraTS 2018, 2019, 2020
[60]	MLBPNN (Machine Learning-Based Back Propagation Neural Networks)	Database - Class I and Class II
[61]	Transfer Learning (TL) and Fine-Tuning (VGG19)	CE-MRI dataset
[63]	Optimized CNN with Ensemble Classification (OCNN-EC)	Kaggle dataset
[64]	NS-EMFSE-CNN, SVM, KNN	TCGA-GBM (Cancer Imaging Archive - TCIA)

3 Brain tumour MRI classification using diverse datasets

Magnetic Resonance Imaging (MRI) plays a pivotal role in the detection, classification, and analysis of brain tumors. Over the years, various datasets have been compiled to aid in the development of automated diagnostic systems. These datasets provide diverse imaging modalities, tumor classifications, and annotations that are crucial for training deep learning models. With the growing advancements in medical imaging and artificial intelligence, the availability of high-quality, labeled datasets has significantly improved brain tumor classification accuracy.

Diversity of brain tumor MRI datasets

Brain tumor MRI datasets vary significantly in terms of size, modalities, and tumor classifications. Some datasets focus on specific tumor types, while others provide a comprehensive collection of images spanning different tumor grades and subtypes.

Publicly available MRI datasets

Several large-scale publicly available datasets have been utilized in brain tumor classification research. The BraTS (Brain Tumor Segmentation) series, including BraTS 2013, 2015, 2017, 2018, 2019, and 2020, remains one of the most widely used datasets. These datasets include MRI scans from patients diagnosed with gliomas, categorized into high-grade gliomas (HGG) and low-grade gliomas (LGG). They contain multimodal imaging sequences, such as T1-weighted, T1 contrast-enhanced (T1ce), T2-weighted, and Fluid-Attenuated Inversion Recovery (FLAIR), which are essential for accurate tumor segmentation and classification. The dataset sizes vary across the years, with the latest versions containing hundreds of training and validation cases.

Other publicly available datasets, such as the Figshare BT dataset, Radiopaedia dataset, and Harvard Medical **dataset**, provide a broader spectrum of brain tumor MRI images. These datasets are particularly useful for multi-class classification tasks, where tumors such as gliomas, meningiomas, and pituitary tumors need to be distinguished. The inclusion of diverse imaging techniques across datasets enhances model generalizability.

Large-Scale MRI collections for brain tumor classification

Some datasets are designed for extensive classification tasks, containing tens of thousands of images. For example, certain datasets include over 110,000 images of gliomas spanning Grade II, III, and IV. Additionally, classification-specific datasets offer thousands of images categorized into multiple tumor types, such as glioblastoma, gliomas, meningiomas, pituitary tumors, and metastatic tumors.

Datasets with such large-scale MRI collections are invaluable for deep learning models, as they provide extensive training data that enables robust classification performance. The MICCAI BraTS 2018 dataset, for instance, contains MRI scans of 220 advanced gliomas and 54 LGG cases, captured across different modalities and resolutions. The Brats 2019 and 2020 datasets further expand this collection, providing 3D images that improve volumetric analysis and classification accuracy.

Multi-Class and multi-modal imaging in MRI classification

Advanced classification models benefit from datasets that offer multi-class labeling and multi-modal imaging. Some datasets, such as the Radiopaedia dataset and BT dataset, include detailed MRI scans categorized into different tumor grades and types. The Cancer Genome Atlas Glioblastoma Multiforme (TCGA-GBM) dataset, available in the TCIA repository, provides T1-Gadolinium (Gd) contrast-enhanced MRI sequences, further aiding in accurate tumor segmentation.

Additionally, datasets with multi-planar MRI images, such as the CE-MRI dataset, offer imaging along axial, coronal, and sagittal planes. These datasets have a 512 × 512-pixel resolution, enabling high-quality tumor identification. The availability of both 2D and 3D datasets allows researchers to experiment with different deep learning architectures, such as convolutional neural networks (CNNs) and 3D-CNN models.

3.1 Challenges in brain tumor MRI classification

Despite the availability of high-quality datasets, brain tumor MRI classification presents several challenges. Variability in tumor shapes, sizes, and locations makes classification difficult, particularly for deep learning models that rely on spatial consistency. Some datasets contain limited annotated data, requiring augmentation techniques to improve training efficiency.

Additionally, the presence of **class imbalance** in some datasets affects model performance. For instance, some datasets have significantly more glioma images than meningiomas or pituitary tumors, leading to biased predictions. Addressing these challenges requires techniques such as data augmentation, transfer learning, and advanced feature extraction.

Role of data augmentation in improving classification accuracy

Data augmentation is an essential technique in MRI-based brain tumor classification. Some datasets, such as the BT dataset, expand their dataset size through augmentation methods, increasing the total number of MRI slices from 3,064 to 91,920. This approach improves the robustness of deep learning models, ensuring better generalization to unseen tumor cases.

Augmentation techniques such as flipping, rotation, contrast adjustment, and Gaussian noise addition enhance dataset diversity. When applied to models trained on smaller datasets, these techniques significantly improve classification accuracy, sensitivity, and specificity.

Performance benchmarks in brain tumor classification

Various classification models have been evaluated using these MRI datasets. Deep learning architectures, such as CNNs, ResNet, and multi-class SVMs, have demonstrated high classification accuracy across different datasets. For instance, classification models trained on Brats 2018 and 2019 datasets achieved accuracy rates of 99.7% for HGG tumors and 98.8% for LGG tumors. Similarly, models trained on the Figshare dataset achieved accuracies exceeding 95% for meningioma, glioma, and pituitary tumor classification.

Other benchmark models, such as Naïve Bayes, K-Nearest Neighbors (KNN), Decision Trees (DT), and Multi-Class SVM, have also been evaluated on datasets like Brats 2013, 2015, 2017, and 2018. The Multi-Class SVM consistently outperformed other models, with accuracy rates above 98% in most cases.

Future directions in brain tumor MRI classification

The future of brain tumor MRI classification lies in the integration of deep learning with advanced medical imaging techniques. The use of transformer-based architectures, hybrid deep learning models, and attention mechanisms has the potential to further enhance classification accuracy. Additionally, federated learning approaches can leverage multi-center datasets while preserving patient privacy, enabling large-scale medical AI applications.

Further research is also needed to improve the interpretability of deep learning models in medical diagnostics. Explainable AI (XAI) techniques can help radiologists understand model decisions, fostering greater adoption of AI-assisted diagnostic tools in clinical settings.

3.2 3D Dataset of brain tumor MRI images

Early tumor detection has been greatly aided in recent years by 3D MRI scans. In this [34] study, The best method for BT segmentation using MRI data is CNN-based 2D U-net segmentation. This method finds regions of interest (ROIs) and trains on all MRI sequences. Normalizing and rescaling input images into 128 × 128 images reduces computing costs and maximizes efficiency. We use 2D layers to combine data. Using the BraTS 2020 brain MRI dataset, this model is trained to determine which of the four MRI sequences achieves the greatest segmentation performance based on MRI image ground truth. The greatest DSC score (93.9%) is achieved using U-Net model T1 MRI sequence training. This study [66] presents 3D Deep dResU-Net, a new method for enhancing BT segmentation accuracy using MRI data. To enhance learning, the U-Net model made use of identity mapping in the encoder, which allowed for the retention of local feature responses and their transmission to the decoder via skip connections. By addressing the issue of the fading gradient, the suggested technique hopes to enhance the training process. Using the BraTS 2020 benchmark dataset, the proposed model was assessed. To ensure the design's resilience, 50 randomly chosen patients from the BraTS 2021 dataset were employed for cross-validation. These cross-validation findings show that the model works well with the external dataset.

To automatically identify the ET, WT, and TC areas in 3D MRI BT images, the author presents a competent approach for segmentation. Positive results were obtained from the studies performed on the BraTS 2020 dataset. By including VNet, the AGSE-VNet model is enhanced. There are total of nine blocks, with five serving as encoders and four as decoders. Each decoder has an Attention Guild Filter block, whereas every encoder has an extrusion and excitation block. With consistent input/output ratios, our model can accommodate such a design without changing the network structure's size discrepancy. The SE module evaluates the model and grants the network access to global data, allowing it to choose relevant data from the enhancement channel. Then, to swiftly boost the model's performance, it uses the Attention Guild Filter block's attention method to capture dependencies. Also added was a new loss function. Change the values of the weights for the unneeded masks in the Categorical_Dice function; for example, make the background region's weight 0.1 and the tumor area of interest's weight 1. Take into consideration the difference between voxels in the background and those in the front [67]. The research study [68] presents a computerized hardware design for segmenting 3D/2D

MRI images, intending to assist professionals in identifying variations in brain tissue for diagnostic purposes. To suggest several solutions to the problems related to the fitness function, position, and velocity, we used a metaheuristic approach based on Particle Swarm Optimization (PSO). The objective is to provide a real-time automated system for segmenting MRI images that increases variables like precision, sensitivity, specificity, execution time, and resource consumption. It demonstrates an 87.97% DSC similarity and executes in a mere 4.57ms using BraTS 2013 brain MRI images. This work [69] utilizes a unique learning strategy to integrate three BT segmentation models that are mutually trained. Mutual Ensemble Learning (MEL) differs from traditional ensemble learning by sharing information across member networks using a novel loss function. Each network is trained using the whole training dataset to ensure comprehensive coverage of strong local minima. Every MEL member network surpasses the performance of the baseline single model, and the ensemble is more resilient. Our MEL has been validated by a thorough examination of two recent BT segmentation datasets. Table 7 provides an elaborate depiction of the 3D MRI BT dataset.

4 Discussion

Through the literature review of many research publications on BT Segmentation and Classification utilizing deep learning (DL) and machine learning (ML) approaches, we could gain a comprehensive grasp of BT diagnosis. The techniques used for brain tissue segmentation include the Hybrid approach using deep convolutional neural networks (DCNNs), UNet architecture, 2DGA-UNet, 3DGA-UNet, VGG-16, and multimodal MRI data. Utilising threshold segmentation, watershed approach, and classifiers for the extraction of BT. Integration of form and texture data to create a merged vector for categorization. The objective of the present research endeavours is to develop a novel architecture, named Attention Gate Residual U-Net (AGResU-Net), for the segmentation of brain tumors (BTs). The proposed architecture aims to improve feature learning and effectively process small-scale BT data by integrating attention gates with residual modules inside a U-Net framework. Achieving precise segmentation of BT regions necessitates the use of many techniques, such as CNN models with a global thresholding strategy, the Daubechies wavelet kernel, and the Partial Differential Diffusion Filter (PDDF). A deep learning approach using convolutional neural networks (CNNs), U-net, transfer learning (TL), and VGG-16 for tumor segmentation and grading enables us to get high accuracy in identifying tumors in Lower-Grade Glioma patients.

The following methods are discussed for BT classification: MLBPNN, infrared sensors, fractal dimension technique, wireless infrared imaging sensor, CNN, grid search optimization, DL strategy, fine-tuning with Temporal Learning, MobilNetV2, INCA feature selection, SVM classification, and CNN with conventional classifiers. The papers provide deep learning techniques for classifying brain tumors using convolutional neural network (CNN) models. The primary objective is to enhance the effectiveness of BT detection via segmentation, classification, and feature extraction. The proposed approach integrates intelligent segmentation, classification, and ensemble classifiers to accurately identify tumors. Non-negative Matrix Factorization (NMF) and Gray Level Co-occurrence Matrix (GLCM) are mathematical methods used to decrease noise and extract pertinent characteristics from MRI images, thereby assisting in precise tumor detection. Furthermore, the work investigates the use of Machine Learning-Based Back Propagation Neural Networks (MLBPNN) to boost diagnostic precision and decrease inconsistency in BT classification, by using infrared sensors for improved picture analysis. The manuscript presents a new transfer learning (TL) technique that utilizes a pre-trained Convolutional Neural Network (CNN) with block-wise fine-tuning to efficiently extract features and classify brain tumours. The Adaptive Fuzzy Deformable Fusion (AFDF) approach achieves improved segmentation accuracy by integrating Fuzzy C-Means Clustering with snake deformable models, which are optimized using the Deer Hunting Optimization Algorithm (DHOA). A novel hybrid Neutrosophy-CNN method is introduced, which combines an ensemble classifier with autoencoder, SVM, and Deep Neural Network to accurately categorize segmented tumor tissues as either benign or malignant.

Subsequently, this article examines the progress made in the early identification of cancers enabled by 3D MRI scans, underscoring the need for precise segmentation techniques for brain tumors detected from MRI data. A novel model, 3D Deep dResU-Net, is presented with the aim of improving the precision of segmentation. To mitigate the problem of fading gradient during training, the encoder utilizes identity mapping to preserve local feature responses. Additionally, the work explores a computerized hardware design for real-time segmentation of 3D/2D MRI images. This design incorporates a Particle Swarm Optimization (PSO) technique to improve accuracy, sensitivity, and processing speed. A novel learning technique named Mutual Ensemble Learning is presented, which combines three BT segmentation models that exchange information across different networks. This methodology guarantees thorough inclusion of local minima and enhances the overall performance.

Some limitations exist in the prior study publications, including despite its success in identifying core and improving tumor regions, the model struggles with low-intensity edema. Due to the ineffective accounting of edema in the model, this shortcoming might result in reduced accuracy in total tumor segmentation. The research uses a two-stage training technique to tackle the data imbalance problem however, this problem might still affect the model's generalizability to new data [30]. The difficulty of creating a functional neural network with fewer computational resources is recognized in the research. Improving the model's segmentation outcomes depends on its capacity to handle more datasets or more complicated pictures, both of which this constraint might

impede [38]. One limitation is that it can't handle dark images, which causes the pre-processing contrast to rise [42]. The reliability of regional forecasts made by TC and ET remains inconsistent [67]. Rather than vast valleys, deep networks may converge into small fissures [69].

.

5 Conclusion

Computer-aided approaches for tumor diagnosis using MRI data may be developed via three processes: BT detection, segmentation, and classification. These approaches provide superior precision, reduced levels of interference, and quicker processing times as compared to manual procedures. Consequently, much research has been conducted on the applications of DL and standard ML technologies. This study investigated several techniques for diagnosing brain MRI images. Additionally, a presentation was given on the comparison of datasets and performance indicators between DL and traditional ML. The overview includes a compilation of three-dimensional datasets that were acquired from a variety of research journals, as well as the approaches that were used to correlate with those datasets. The performance measurements that they have provided evidence of the best accuracy rate. Following that comes the discussion section, which provides a concise summary of the whole work and outlines the constraints of the research. Although significant advancements have been made in tumor diagnosis using MRI-based automated approaches, there are several areas for future research. One key direction is enhancing model generalization across diverse MRI datasets by incorporating transfer learning and domain adaptation techniques. Additionally, integrating multi-modal imaging data, such as combining MRI with PET or CT scans, may improve diagnostic accuracy and robustness. Further research could explore the interpretability and explainability of deep learning models to increase clinical trust and acceptance. The development of lightweight, real-time models suitable for deployment in low-resource clinical settings is another promising avenue. Finally, improving data augmentation and preprocessing techniques to handle class imbalance and noise in medical images can further refine model performance and reliability.

References

[1] J. Amin, M. Sharif, A. Haldorai, M. Yasmin, and R. S. Nayak, “Brain tumor detection and classification using machine learning: a comprehensive survey,” *Complex Intell. Syst.*, vol. 8, no. 4, pp. 3161–3183, 2022, doi: 10.1007/s40747-021-00563-y.

[2] W. Ayadi, W. Elhamzi, I. Charfi, and M. Atri, “Deep CNN for Brain Tumor Classification,” *Neural Process. Lett.*, vol. 53, no. 1, pp. 671–700, 2021, doi: 10.1007/s11063-020-10398-2.

[3] M. I. Sharif, J. P. Li, J. Amin, and A. Sharif, “An improved framework for brain tumor analysis using MRI based on YOLOv2 and convolutional neural network,” *Complex Intell. Syst.*, vol. 7, no. 4, pp. 2023–2036, 2021, doi: 10.1007/s40747-021-00310-3.

[4] M. K. Abd-Ellah, A. I. Awad, A. A. M. Khalaf, and H. F. A. Hamed, “A review on brain tumor diagnosis from MRI images: Practical implications, key achievements, and lessons learned,” *Magn. Reson. Imaging*, vol. 61, no. August 2018, pp. 300–318, 2019, doi: 10.1016/j.mri.2019.05.028.

[5] M. Nazir, S. Shakil, and K. Khurshid, “Role of deep learning in brain tumor detection and classification (2015 to 2020): A review,” *Comput. Med. Imaging Graph.*, vol. 91, no. April, 2021, doi: 10.1016/j.compmedimag.2021.101940.

[6] A. Maier, C. Syben, T. Lasser, and C. Riess, “A gentle introduction to deep learning in medical image processing,” *Z. Med. Phys.*, vol. 29, no. 2, pp. 86–101, 2019, doi: 10.1016/j.zemedi.2018.12.003.

[7] K. R. Bhatele and S. S. Bhadauria, “Brain structural disorders detection and classification approaches: a review,” *Artif. Intell. Rev.*, vol. 53, no. 5, pp. 3349–3401, 2020, doi: 10.1007/s10462-019-09766-9.

[8] M. I. Sharif, J. P. Li, J. Naz, and I. Rashid, “A comprehensive review on multi-organs tumor detection based on machine learning,” *Pattern Recognit. Lett.*, vol. 131, pp. 30–37, 2020, doi: 10.1016/j.patrec.2019.12.006.

[9] S. S. Begum and D. R. Lakshmi, “Combining optimal wavelet statistical texture and recurrent neural network for tumour detection and classification over MRI,” *Multimed. Tools Appl.*, vol. 79, no. 19–20, pp. 14009–14030, 2020, doi: 10.1007/s11042-020-08643-w.

[10] J. Amin, M. Sharif, M. Raza, T. Saba, R. Sial, and S. A. Shad, “Brain tumor detection: a long short-term memory (LSTM)-based learning model,” *Neural Comput. Appl.*, vol. 32, no. 20, pp. 15965–15973, 2020, doi: 10.1007/s00521-019-04650-7.

[11] T. Saba *et al.*, “Brain tumor detection using fusion of hand crafted and deep learning features,” *Cogn. Syst. Res.*, vol. 59, pp. 221–230, 2020, doi: 10.1016/j.cogsys.2019.09.007.

[12] J. Amin, M. Sharif, M. Yasmin, and S. L. Fernandes, “A distinctive approach in brain tumor detection and classification using MRI,” *Pattern Recognit. Lett.*, vol. 139, pp. 118–127, 2020, doi: 10.1016/j.patrec.2017.10.036.

[13] M. Sharif, J. Amin, M. W. Nisar, M. A. Anjum, N. Muhammad, and S. Ali Shad, “A unified patch-based method for brain tumor detection using features fusion,” *Cogn. Syst. Res.*, vol. 59, pp. 273–286, 2020, doi: 10.1016/j.cogsys.2019.10.001.

[14] M. I. Sharif, J. P. Li, M. A. Khan, and M. A. Saleem, “Active deep neural network features selection for segmentation and recognition of brain tumors using MRI images,” *Pattern Recognit. Lett.*, vol. 129, pp. 181–189, 2020, doi: 10.1016/j.patrec.2019.11.019.

[15] M. Sharif, J. Amin, M. Raza, M. Yasmin, and S. C. Satapathy, “An integrated design of particle swarm optimization (PSO) with fusion of features for detection of brain tumor,” *Pattern Recognit. Lett.*, vol. 129, pp. 150–157, 2020, doi: 10.1016/j.patrec.2019.11.017.

[16] J. Amin, M. Sharif, N. Gul, M. Yasmin, and S. A. Shad, "Brain tumor classification based on DWT fusion of MRI sequences using convolutional neural network," *Pattern Recognit. Lett.*, vol. 129, pp. 115–122, 2020, doi: 10.1016/j.patrec.2019.11.016.

[17] J. Chang *et al.*, "A mix-pooling CNN architecture with FCRF for brain tumor segmentation," *J. Vis. Commun. Image Represent.*, vol. 58, pp. 316–322, 2019, doi: 10.1016/j.jvcir.2018.11.047.

[18] K. R. M. Fernando and C. P. Tsokos, "Deep and statistical learning in biomedical imaging: State of the art in 3D MRI brain tumor segmentation," *Inf. Fusion*, vol. 92, no. August 2022, pp. 450–465, 2023, doi: 10.1016/j.inffus.2022.12.013.

[19] A. Elazab *et al.*, "GP-GAN: Brain tumor growth prediction using stacked 3D generative adversarial networks from longitudinal MR Images," *Neural Networks*, vol. 132, pp. 321–332, 2020, doi: 10.1016/j.neunet.2020.09.004.

[20] M. Mazzei, "A Change Detection with Machine Learning Approach for Medical Image Analysis," *Lect. Notes Electr. Eng.*, vol. 810 LNEE, no. December, pp. 203–229, 2023, doi: 10.1007/978-981-16-6775-6_18.

[21] W. Ayadi, W. Elhamzi, I. Charfi, and M. Atri, "A hybrid feature extraction approach for brain MRI classification based on Bag-of-words," *Biomed. Signal Process. Control*, vol. 48, pp. 144–152, 2019, doi: 10.1016/j.bspc.2018.10.010.

[22] M. Puttagunta and S. Ravi, "Medical image analysis based on deep learning approach," *Multimed. Tools Appl.*, vol. 80, no. 16, pp. 24365–24398, 2021, doi: 10.1007/s11042-021-10707-4.

[23] K. R. M. Fernando and C. P. Tsokos, "Deep and statistical learning in biomedical imaging: State of the art in 3D MRI brain tumor segmentation," *Inf. Fusion*, vol. 92, no. November 2022, pp. 450–465, 2023, doi: 10.1016/j.inffus.2022.12.013.

[24] C. Sundar and R. K. Karunakara, "Efficient Detection and Classification of Brain Tumor using Kernel based SVM for MRI," *Multimed. Tools Appl.*, pp. 7393–7417, 2022, doi: 10.1007/s11042-021-11821-z.

[25] J. Amin, M. Sharif, M. Yasmin, T. Saba, and M. Raza, "Use of machine intelligence to conduct analysis of human brain data for detection of abnormalities in its cognitive functions," *Multimed. Tools Appl.*, vol. 79, no. 15–16, pp. 10955–10973, 2020, doi: 10.1007/s11042-019-7324-y.

[26] J. Jayashree and S. A. Kumar, "Linear Discriminant Analysis Based Genetic Algorithm with Generalized Regression Neural Network – A Hybrid Expert System for Diagnosis of Diabetes," *Program. Comput. Softw.*, vol. 44, no. 6, pp. 417–427, 2018, doi: 10.1134/S0361768818060063.

[27] A. Kabir Anaraki, M. Ayati, and F. Kazemi, "Magnetic resonance imaging-based brain tumor grades classification and grading via convolutional neural networks and genetic algorithms," *Biocybern. Biomed. Eng.*, vol. 39, no. 1, pp. 63–74, 2019, doi: 10.1016/j.bbe.2018.10.004.

[28] J. Jayashree and S. Ananda Kumar, "Hybrid swarm intelligent redundancy relevance (RR) with convolution trained compositional pattern neural network expert system for diagnosis of diabetes," *Health Technol. (Berl).*, vol. 10, no. 1, pp. 197–206, 2020, doi: 10.1007/s12553-018-00291-3.

[29] J. Jayashree and S. Ananda Kumar, "Evolutionary correlated gravitational search algorithm (ECGS) with genetic optimized Hopfield neural network (GHNN) – A hybrid expert system for diagnosis of diabetes," *Meas. J. Int. Meas. Confed.*, vol. 145, pp. 551–558, 2019, doi: 10.1016/j.measurement.2018.12.083.

[30] S. Sajid, S. Hussain, and A. Sarwar, "Brain Tumor Detection and Segmentation in MR Images Using Deep Learning," *Arab. J. Sci. Eng.*, vol. 44, no. 11, pp. 9249–9261, 2019, doi: 10.1007/s13369-019-03967-8.

[31] J. Amin *et al.*, "Brain Tumor Detection by Using Stacked Autoencoders in Deep Learning," *J. Med. Syst.*, vol. 44, no. 2, 2020, doi: 10.1007/s10916-019-1483-2.

[32] A. Kaur, L. Kaur, and A. Singh, *GA-UNet: UNet-based framework for segmentation of 2D and 3D medical images applicable on heterogeneous datasets*, vol. 33, no. 21. Springer London, 2021. doi: 10.1007/s00521-021-06134-z.

[33] Z. Shaukat, Q. ul A. Farooq, S. Tu, C. Xiao, and S. Ali, "A state-of-the-art technique to perform cloud-based semantic segmentation using deep learning 3D U-Net architecture," *BMC Bioinformatics*, vol. 23, no. 1, pp. 1–21, 2022, doi: 10.1186/s12859-022-04794-9.

[34] S. Montaha, S. Azam, A. K. M. Rakibul Haque Rafid, M. Z. Hasan, and A. Karim, "Brain Tumor Segmentation from 3D MRI Scans Using U-Net," *SN Comput. Sci.*, vol. 4, no. 4, pp. 1–10, 2023, doi: 10.1007/s42979-023-01854-6.

[35] J. Zhang, Z. Jiang, J. Dong, Y. Hou, and B. Liu, "Attention Gate ResU-Net for Automatic MRI Brain Tumor Segmentation," *IEEE Access*, vol. 8, pp. 58533–58545, 2020, doi: 10.1109/ACCESS.2020.2983075.

[36] M. A. Naser and M. J. Deen, "Brain tumor segmentation and grading of lower-grade glioma using deep learning in MRI images," *Comput. Biol. Med.*, vol. 121, no. February, 2020, doi: 10.1016/j.compbiomed.2020.103758.

[37] G. Karayegen and M. F. Aksahin, "Brain tumor prediction on MR images with semantic segmentation by using deep learning network and 3D imaging of tumor region," *Biomed. Signal Process. Control*, vol. 66, no. January, 2021, doi: 10.1016/j.bspc.2021.102458.

[38] J. Sun, Y. Peng, Y. Guo, and D. Li, "Segmentation of the multimodal brain tumor image used the multi-pathway architecture method based on 3D FCN," *Neurocomputing*, vol. 423, pp. 34–45, 2021, doi: 10.1016/j.neucom.2020.10.031.

[39] P. Agrawal, N. Katal, and N. Hooda, "Segmentation and classification of brain tumor using 3D-UNet

deep neural networks," *Int. J. Cogn. Comput. Eng.*, vol. 3, no. August 2021, pp. 199–210, 2022, doi: 10.1016/j.ijcce.2022.11.001.

[40] V. V. S. Sasank and S. Venkateswarlu, "An automatic tumour growth prediction-based segmentation using full resolution convolutional network for brain tumour," *Biomed. Signal Process. Control*, vol. 71, no. April 2021, 2022, doi: 10.1016/j.bspc.2021.103090.

[41] J. Liu *et al.*, "IOUC-3DSFCNN: Segmentation of Brain Tumors via IOU Constraint 3D Symmetric Full Convolution Network with Multimodal Auto-context," *Sci. Rep.*, vol. 10, no. 1, pp. 1–15, 2020, doi: 10.1038/s41598-020-63242-x.

[42] H. Habib, R. Amin, B. Ahmed, and A. Hannan, "Hybrid algorithms for brain tumor segmentation, classification and feature extraction," *J. Ambient Intell. Humaniz. Comput.*, vol. 13, no. 5, pp. 2763–2784, 2022, doi: 10.1007/s12652-021-03544-8.

[43] H. Mzoughi *et al.*, "Deep Multi-Scale 3D Convolutional Neural Network (CNN) for MRI Gliomas Brain Tumor Classification," *J. Digit. Imaging*, vol. 33, no. 4, pp. 903–915, 2020, doi: 10.1007/s10278-020-00347-9.

[44] S. Deepak and P. M. Ameer, "Automated Categorization of Brain Tumor from MRI Using CNN features and SVM," *J. Ambient Intell. Humaniz. Comput.*, vol. 12, no. 8, pp. 8357–8369, 2021, doi: 10.1007/s12652-020-02568-w.

[45] M. I. Sharif, M. A. Khan, M. Alhussein, K. Aurangzeb, and M. Raza, "A decision support system for multimodal brain tumor classification using deep learning," *Complex Intell. Syst.*, vol. 8, no. 4, pp. 3007–3020, 2022, doi: 10.1007/s40747-021-00321-0.

[46] E. Irmak, "Multi-Classification of Brain Tumor MRI Images Using Deep Convolutional Neural Network with Fully Optimized Framework," *Iran. J. Sci. Technol. - Trans. Electr. Eng.*, vol. 45, no. 3, pp. 1015–1036, 2021, doi: 10.1007/s40998-021-00426-9.

[47] M. I. Sharif, J. P. Li, M. A. Khan, S. Kadry, and U. Tariq, "M3BTCNet: multi model brain tumor classification using metaheuristic deep neural network features optimization," *Neural Comput. Appl.*, vol. 36, no. 1, pp. 95–110, 2024, doi: 10.1007/s00521-022-07204-6.

[48] M. Li, L. Kuang, S. Xu, and Z. Sha, "Brain Tumor Detection Based on Multimodal Information Fusion and Convolutional Neural Network," *IEEE Access*, vol. 7, pp. 180134–180146, 2019, doi: 10.1109/ACCESS.2019.2958370.

[49] S. Montaha, S. Azam, A. K. M. R. H. Rafid, M. Z. Hasan, A. Karim, and A. Islam, "TimeDistributed-CNN-LSTM: A Hybrid Approach Combining CNN and LSTM to Classify Brain Tumor on 3D MRI Scans Performing Ablation Study," *IEEE Access*, vol. 10, pp. 60039–60059, 2022, doi: 10.1109/ACCESS.2022.3179577.

[50] M. Sajjad, S. Khan, K. Muhammad, W. Wu, A. Ullah, and S. W. Baik, "Multi-grade brain tumor classification using deep CNN with extensive data augmentation," *J. Comput. Sci.*, vol. 30, pp. 174–182, 2019, doi: 10.1016/j.jocs.2018.12.003.

[51] H. Shahamat and M. Saniee Abadeh, "Brain MRI analysis using a deep learning based evolutionary approach," *Neural Networks*, vol. 126, pp. 218–234, 2020, doi: 10.1016/j.neunet.2020.03.017.

[52] S. Ali, A. Ismael, A. Mohammed, and H. Hefny, "Arti fi cial Intelligence In Medicine An enhanced deep learning approach for brain cancer MRI images classi fi cation using residual networks," vol. 102, no. December 2019, 2020.

[53] A. Akter *et al.*, "Robust clinical applicable CNN and U-Net based algorithm for MRI classification and segmentation for brain tumor," *Expert Syst. Appl.*, vol. 238, no. October 2023, 2024, doi: 10.1016/j.eswa.2023.122347.

[54] J. Vaishnavi, S. Ravi, and A. Anbarasi, "An efficient adaptive histogram-based segmentation and extraction model for the classification of severities on diabetic retinopathy," *Multimed. Tools Appl.*, vol. 79, no. 41–42, pp. 30439–30452, 2020, doi: 10.1007/s11042-020-09288-5.

[55] C. Öksüz, O. Urhan, and M. K. Güllü, "Brain tumor classification using the fused features extracted from expanded tumor region," *Biomed. Signal Process. Control*, vol. 72, no. September 2020, 2022, doi: 10.1016/j.bspc.2021.103356.

[56] A. Kursad Poyraz, S. Dogan, E. Akbal, and T. Tuncer, "Automated brain disease classification using exemplar deep features," *Biomed. Signal Process. Control*, vol. 73, no. December 2021, 2022, doi: 10.1016/j.bspc.2021.103448.

[57] A. Chattopadhyay and M. Maitra, "MRI-based brain tumour image detection using CNN based deep learning method," *Smart Agric. Technol.*, vol. 2, no. 4, 2022, doi: 10.1016/j.neuri.2022.100060.

[58] N. F. Aurna, M. A. Yousuf, K. A. Taher, A. K. M. Azad, and M. A. Moni, "A classification of MRI brain tumor based on two stage feature level ensemble of deep CNN models," *Comput. Biol. Med.*, vol. 146, no. April, 2022, doi: 10.1016/j.compbiomed.2022.105539.

[59] F. Demir, Y. Akbulut, B. Taşcı, and K. Demir, "Improving brain tumor classification performance with an effective approach based on new deep learning model named 3ACL from 3D MRI data," *Biomed. Signal Process. Control*, vol. 81, no. October 2022, 2023, doi: 10.1016/j.bspc.2022.104424.

[60] P. M. Shakeel, T. E. E. L. Tobely, H. Al-feel, G. Manogaran, and S. Baskar, "Neural Network Based Brain Tumor Detection Using Wireless Infrared Imaging Sensor," *IEEE Access*, vol. 7, pp. 5577–5588, 2019, doi: 10.1109/ACCESS.2018.2883957.

[61] Z. N. K. Swati *et al.*, "Brain tumor classification for MR images using transfer learning and fine-tuning," *Comput. Med. Imaging Graph.*, vol. 75, pp. 34–46, 2019, doi: 10.1016/j.compmedimag.2019.05.001.

[62] J. Amin, M. Sharif, M. Yasmin, T. Saba, M. A. Anjum, and S. L. Fernandes, "A New Approach for

Brain Tumor Segmentation and Classification Based on Score Level Fusion Using Transfer Learning," *J. Med. Syst.*, vol. 43, no. 11, 2019, doi: 10.1007/s10916-019-1453-8.

[63] M. Y. B. Murthy, A. Koteswararao, and M. S. Babu, "Adaptive fuzzy deformable fusion and optimized CNN with ensemble classification for automated brain tumor diagnosis," *Biomed. Eng. Lett.*, vol. 12, no. 1, pp. 37–58, 2022, doi: 10.1007/s13534-021-00209-5.

[64] F. Özyurt, E. Sert, E. Avci, and E. Dogantekin, "Brain tumor detection based on Convolutional Neural Network with neutrosophic expert maximum fuzzy sure entropy," vol. 147, 2019.

[65] C. Narmatha, S. M. Eljack, A. A. R. M. Tuka, S. Manimurugan, and M. Mustafa, "A hybrid fuzzy brain-storm optimization algorithm for the classification of brain tumor MRI images," *J. Ambient Intell. Humaniz. Comput.*, no. 0123456789, 2020, doi: 10.1007/s12652-020-02470-5.

[66] R. Raza, U. Ijaz Bajwa, Y. Mehmood, M. Waqas Anwar, and M. Hassan Jamal, "dResU-Net: 3D deep residual U-Net based brain tumor segmentation from multimodal MRI," *Biomed. Signal Process. Control*, vol. 79, no. P1, p. 103861, 2023, doi: 10.1016/j.bspc.2022.103861.

[67] X. Guan *et al.*, "3D AGSE-VNet: an automatic brain tumor MRI data segmentation framework," *BMC Med. Imaging*, vol. 22, no. 1, pp. 1–18, 2022, doi: 10.1186/s12880-021-00728-8.

[68] F. Hamdaoui and A. Sakly, "Automatic diagnostic system for segmentation of 3D/2D brain MRI images based on a hardware architecture," *Microprocess. Microsyst.*, vol. 98, no. February, 2023, doi: 10.1016/j.micpro.2023.104814.

[69] J. Hu, X. Gu, and X. Gu, "Mutual ensemble learning for brain tumor segmentation," *Neurocomputing*, vol. 504, pp. 68–81, 2022, doi: 10.1016/j.neucom.2022.06.058.